Caving 2026 – A van As, D Cumming-Potvin & J Wesseloo (eds)

doi:10.36487/ACG_repo/2645_48

# Caving monitoring with integrated fibre-optic acoustic and strain sensing: a field experiment

**Qingdong Qu [a,*], Joey Duan [a], Karsten Hoehn [a], Xulu Lin [a], Dale Harpley [a], Matt van de Werken [a]**

[a] *CSIRO Mineral Resources, Australia*

## Abstract

*Reliable monitoring of rock mass conditions is critical to ensuring safe and efficient resource extraction using the underground caving method, particularly under complex geological and mining conditions. Distributed fibre-optic sensing, with its spatially dense measurement capabilities, shows high potential for capturing detailed insights into rock mass deformation and fracturing activities, especially in the vertical direction.*

*This paper presents a field experiment on monitoring rock mass fracturing and deformation propagation using an integrated distributed acoustic sensing (DAS) and distributed strain sensing (DSS) approach. Fibre-optic cables were installed in two surface boreholes and a surface trench, along with two geophones in each borehole for validation. Monitoring data were continuously acquired over a 10-month period, during which extensive seismic activity was recorded. The inferred rock mass deformation and fracturing activities are consistent with conventional understanding while revealing additional information that can complement geotechnical assessment. The trial also demonstrated the capability to detect low-magnitude events at specific depth intervals to support assessment of weak zone behaviour.*

**Keywords:** *caving, distributed fibre-optic sensing, distributed acoustic sensing, distributed strain sensing, subsidence*

## 1 Introduction

Caving mining is increasingly being adopted to meet the growth in global demand for mineral resources as ore grades decline and mining depths increase. Safe and efficient caving operations rely on timely and reliable monitoring of rock mass responses during extraction. Inadequate monitoring can lead to poor cave management, resulting in elevated geotechnical risks, reduced extraction efficiency and increased dilution.

A range of monitoring techniques is commonly employed in caving operations, including microseismic systems, extensometers, open hole dipping and smart markers. These techniques provide valuable information on assessing rock damage, deformation behaviour, cave propagation, surface subsidence and cave flow dynamics, supporting geotechnical management and draw strategy optimisation.

In recent years, distributed fibre-optic sensing (DFOS) technology, which has been widely used in the oil and gas industry, has been increasingly developed and trialled in underground caving applications such as longwall panels, sublevel caving and block caving mines. DFOS offers unique advantages of continuous, high spatial resolution sensing of rock mass condition changes along the full length of installed fibre-optic cables. Previous studies have demonstrated the capability of DAS to detect mining-induced microseismicity in both underground coal and metal mines (Luo and Duan, 2021, du Toit et al., 2022, Duan et al., 2023; 2025, Dande et al., 2024). In addition, DSS has been successfully applied in various mines to monitor deformation and caving propagation as mining progresses (Xie et al., 2023, John and Hoehn, 2024).

In these applications, DAS and DSS have typically been applied independently. Integrating both techniques would provide complementary information on rock mass fracturing and deformation, greatly enhancing

[*] Corresponding author. Email address: qingdong.qu@csiro.au

interpretability with only marginal additional cost. This paper presents a field experiment demonstrating the integrated application of DAS and DSS for monitoring mining-induced rock mass fracturing processes.

# 2 Design and field experiment

## 2.1 Design principles

The conceptual model proposed by Duplancic & Brady (1999) and its subsequent modifications is widely used to interpret caving mechanisms and propagation (Figure 1). The model defines five distinct rock mass behaviour zones: the caved zone, airgap, yield zone, seismogenic zone and elastic zone, with microseismic activity predominantly occurring within the seismogenic zone.

Following caving initiation, progressive failure of the rock mass drives the upward migration of the seismogenic zone, enabling caving propagation to be assessed through microseismic monitoring. With fibre-optic cables installed in boreholes, DAS provides spatially dense and continuous recording of the strain rate associated with microseismic events along the entire cable length, allowing more accurate determination of microseismic events at depth and more reliable estimation of seismogenic zone migration. When further integrated with geophones, the approach can enhance characterisation of seismic source parameters and estimation of seismic magnitude.

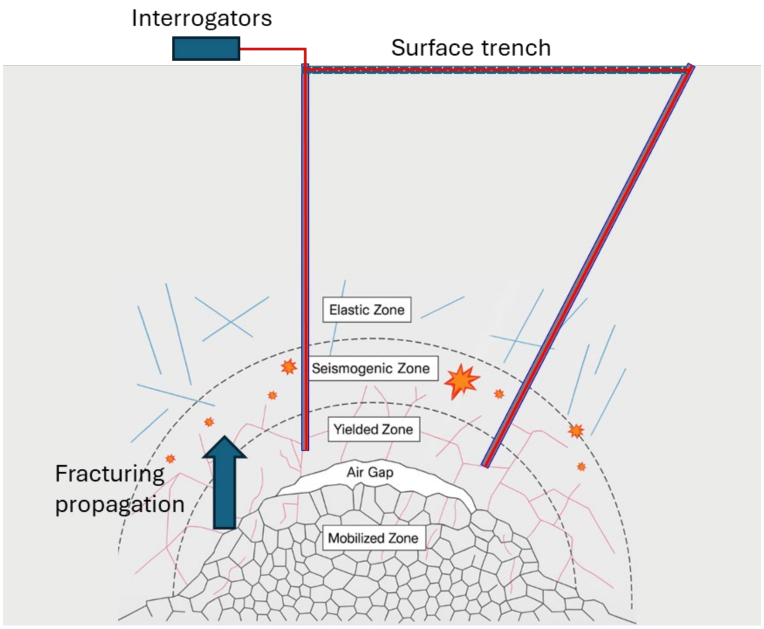


**Figure 1 Conceptual design of an integrated DAS-DSS system based on a typical caving model (modified from Sainsbury 2012 and after Duplancic & Brady 1999). Boreholes may be drilled vertically or inclined, depending on surface access conditions. Effective caving monitoring requires 2–3 holes**

As caving progresses, the yielded and seismogenic zones expand, resulting in stress redistribution and the development of a dynamic deformation zone around the cave. This deformation may extend beyond the area directly above the footprint. A fibre-optic cable installed in a borehole intersecting the propagating deformation zone can provide continuous measurements of strain evolution, offering insight into stress redistribution and deformation processes. This behaviour is observed in both block caving and longwall mining. For example, Figure 2 shows strain development along a cable installed above a longwall mining panel as the face advanced past the instrument borehole. The progressive strain initiation, development and eventual cable breakage indicate the evolution of stress redistribution and rock mass deformation.

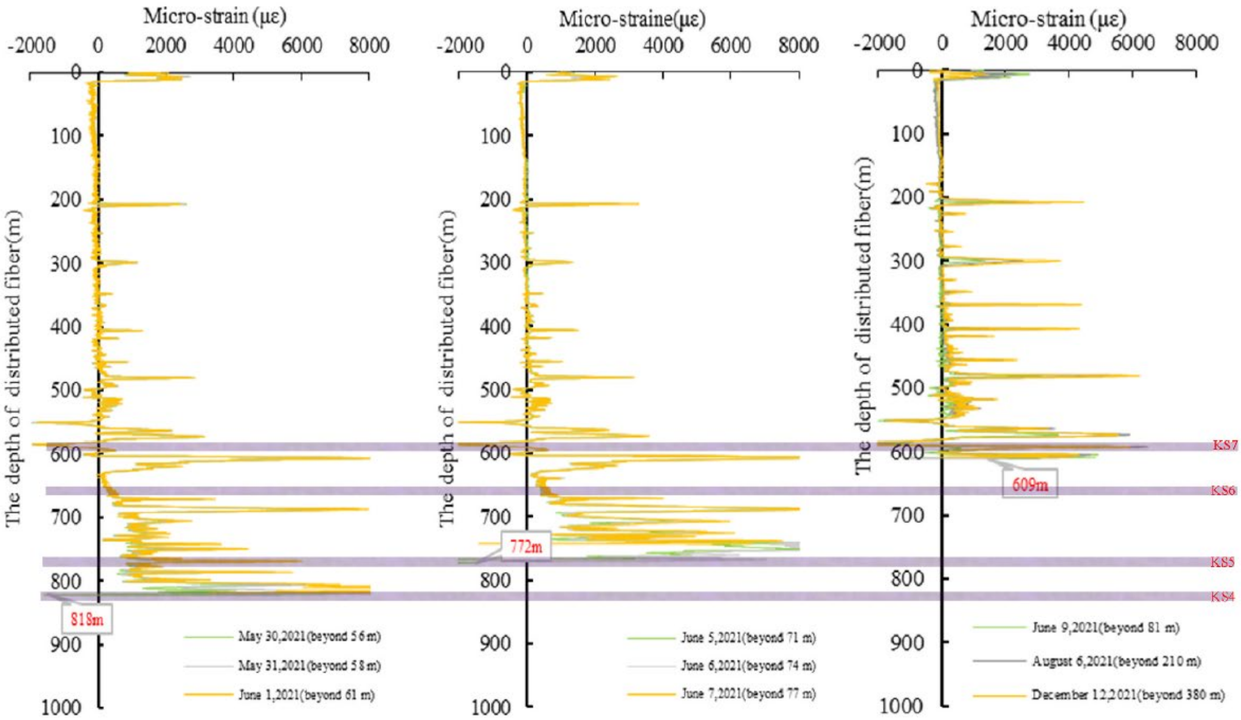


**Figure 2 DSS-measured overburden strain development above a longwall caving panel as the longwall face advanced past the instrument hole by different distances (Xie et al. 2023)**

## 2.2 Field installation

Based on the above design principles, an integrated DAS-DSS system was deployed at a caving mine using two existing inclined surface boreholes. The two holes were drilled from outside the surface subsidence zone towards the cave footprint, with original lengths of 510 m (Hole 1) and 450 m (Hole 2). At the time of installation, Hole 1 had already broken through to its expected final position (approximately 410 m) on the cave edge, whereas Hole 2 remained intact along its full drill length. Hole 2 was expected to break through to its length of approximately 300 m as caving progressed. The extraction level is located at approximately 500 m below the ground surface.

Two types of fibre-optic cables, a loose tube cable and a tight buffer mil-spec breakout cable, were installed in each borehole, along with three triaxial geophones per borehole location (two in the hole and one near the surface collar) to enable cross-validation of DAS measurements. The loose tube cable was used specifically for DAS while the tight buffer mil-spec cable was used for DSS. A surface trench was excavated to connect the fibre cables from the two boreholes to form continuous fibres for both DAS and DSS. This configuration allows the use of a single interrogator for DAS and a single interrogator for DSS, minimising the number of interrogators required and improving cost efficiency. Borehole collars were located to the east and northwest of the cave and drilled towards the centre of the footprint. Figure 3 illustrates the fibre-optic cable and geophone configuration installed in the two boreholes.

The DFOS system operated for over 10 months and remained largely stable throughout the monitoring period. Minor interruptions occurred due to power outages and occasional fibre damage from wildlife interference. The geophones were recording continuously for the entire monitoring period.

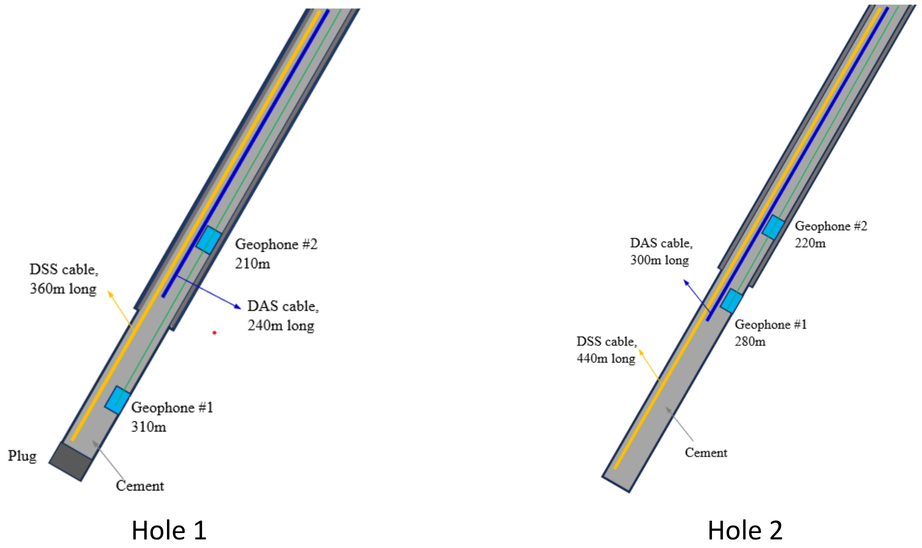


**Figure 3 Schematic of the borehole fibre-optic cable and geophone configuration**

# 3 DAS results

## 3.1 Data processing

The DAS system was configured with a channel spacing of 4 m and a sampling rate of 500 Hz. Because DAS measures axial strain rate along the fibre cable, it is crucial to enhance the signal-to-noise ratio. Frequency–wavenumber analysis suggested that the main coherent noise frequencies registered at the mine were around 35 Hz and 60 Hz. Accordingly, band-stop filters were applied to remove coherent noise. A low-pass filter was also used to reject higher frequency signal components, as the dominant seismic frequency was below 100 Hz (Figure 4).

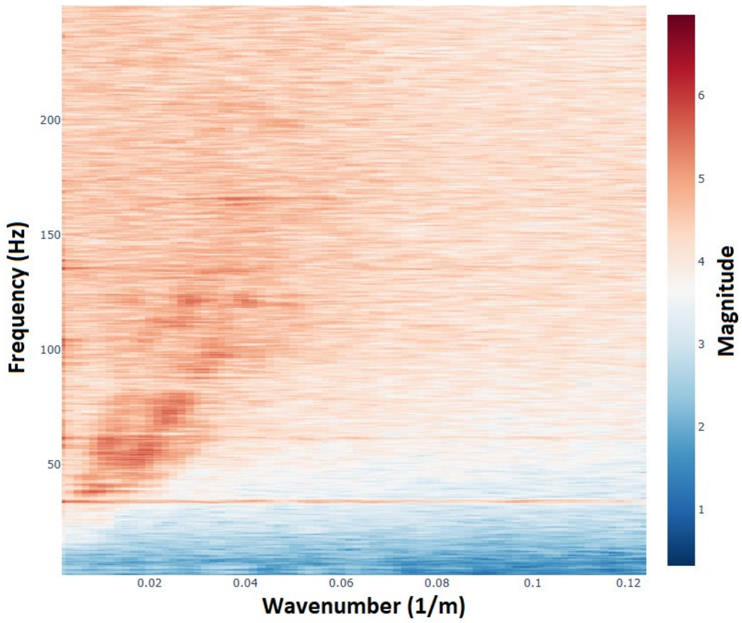


**Figure 4 Frequency–wavenumber spectrum associated with a seismic event recorded by DAS**

Figure 5 shows a representative DAS wavefield of a recorded microseismic event. These events are associated with typical shear failures of rock mass. P-waves and S-waves were clearly captured by the fibre-optic cables. They exhibited large amplitude, which can be reliably discriminated. The wavefield recorded by the fibre cable installed in the trench on ground surface is also shown in this figure. As the trench was backfilled with loose soil, the coupling between the fibre cable and the ground was not suitable for monitoring the seismic activity. Strong scattering of surface waves can be observed due to strong attenuation and near-surface heterogeneity.

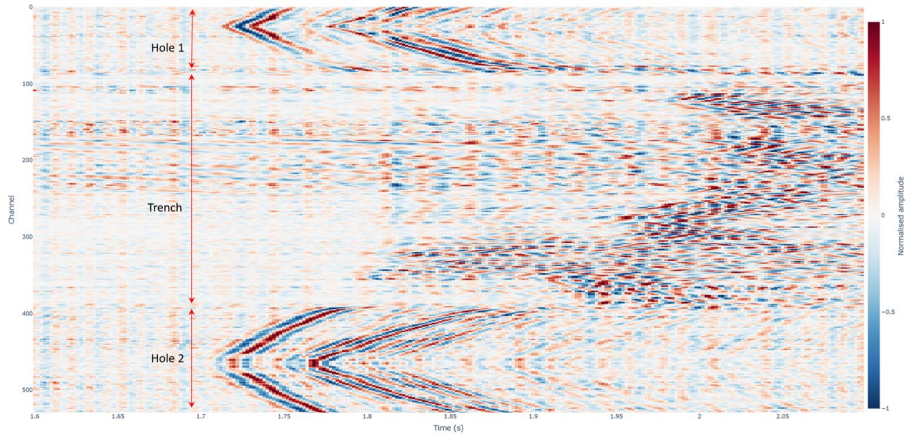


**Figure 5 Example DAS wavefields of a typical strong seismic event clearly recorded along the fibre cables in both holes. Image shows the fibre cables installed in the two boreholes only**

The seismic velocity model was derived and calibrated with multiple blasting events at the mine. The high-energy blast signals enabled clear identification of P-wave arrivals across the DAS network. The differences in arrival times and distances from the source to the DAS channels in the two holes were calculated to estimate the average P-wave velocity (Figure 6), which was subsequently used for event location. The S-wave velocity was derived from an empirical P-wave to S-wave velocity ratio of 1.73.

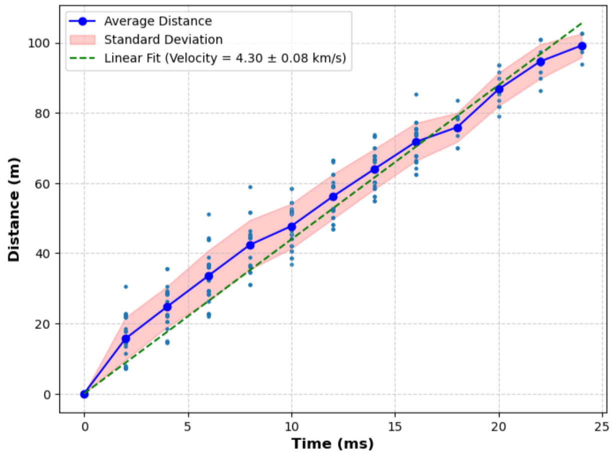


**Figure 6 Average P-wave velocity obtained using mine blasts**

Local magnitudes were estimated by calibrating DAS responses against collocated reference geophones installed in each borehole. Local magnitude scale $M_L$ was obtained using the following equation:

$$M_L = \log A - \log A_0 + S \quad (1)$$

where:

$A$ = critical the maximum amplitude of the body wave on the horizontal components of the geophone

$S$ = critical empirical station correction terms

$\log A_0$= critical reference amplitude related to the distance between the seismic event and the geophone.

As two triaxial geophones were installed alongside the fibre cable in each of two boreholes, the maximum amplitudes recorded by the horizontal components of each geophone were used to derive the local magnitudes.

Local magnitudes were used to maintain consistency with practices at the mine, as well as for enabling rapid estimation with sparse distribution of installed geophones. Although more rigorous quantification of source parameters could be performed using moment magnitude analysis, the primary aim of this study was to evaluate the feasibility of DAS for monitoring fracture propagation during caving. Therefore, simplified local magnitudes were considered sufficient for this purpose.

## 3.2 Characteristics of microseismic events

Over the monitoring period, a total of 5,104 seismic triggers were identified by the DAS system, with typical daily counts ranging from 10 to 50 during normal production (Figure 7). This trigger rate appears to be lower than rates reported in other studies; however, this might reflect site-specific conditions.

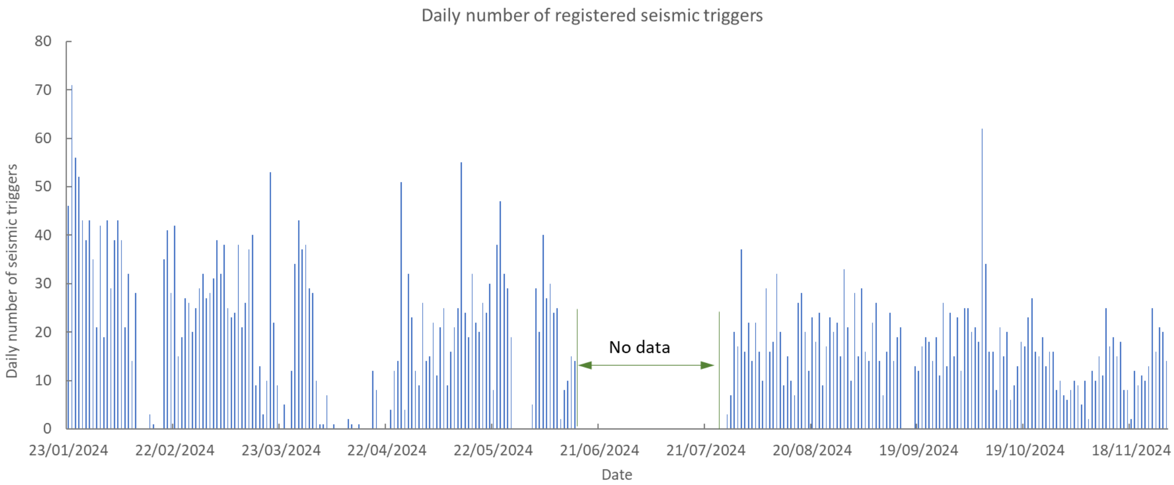


**Figure 7 Daily number of seismic triggers over the monitoring period. The monitoring was interrupted from late Jue to early August due to power outages and fibre cable disconnections. No data processing was performed during this period**

Of the recorded seismic triggers, 1,004 were located using the calibrated velocity model and the local magnitudes were estimated. The posterior location uncertainties of seismic events were evaluated, and only events with location errors below 30 m were accepted. As a result, approximately 80% of seismic triggers could not be reliably located. As shown in Figure 8, these events do not show clear signal-to-noise ratios, making it difficult to reliably pick first arrivals for source location.

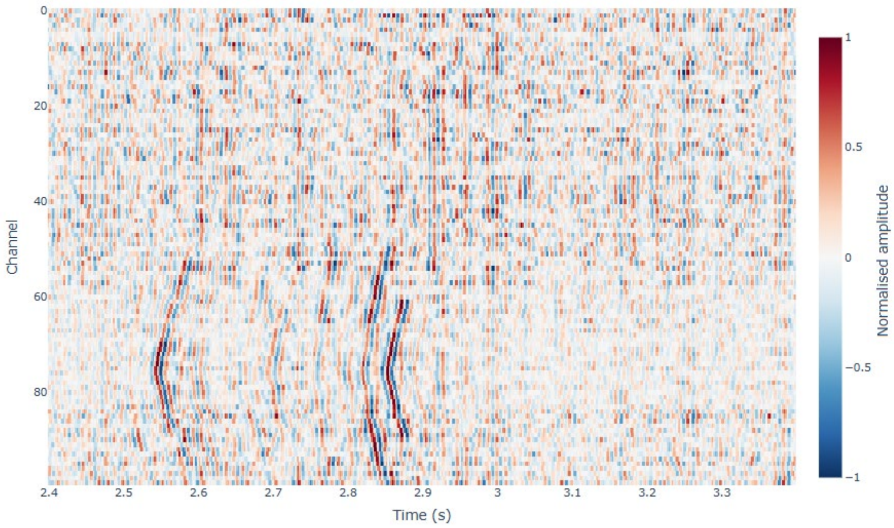


**Figure 8 Example of DAS wavefield of a seismic trigger which was rejected for source location**

As shown in Figure 9, estimated local magnitudes primarily ranged from −3 to –1, with the largest local magnitude of −0.8. This local magnitude range is consistent with magnitudes of caving-induced seismicity recorded by other microseismic monitoring systems at the study mine.

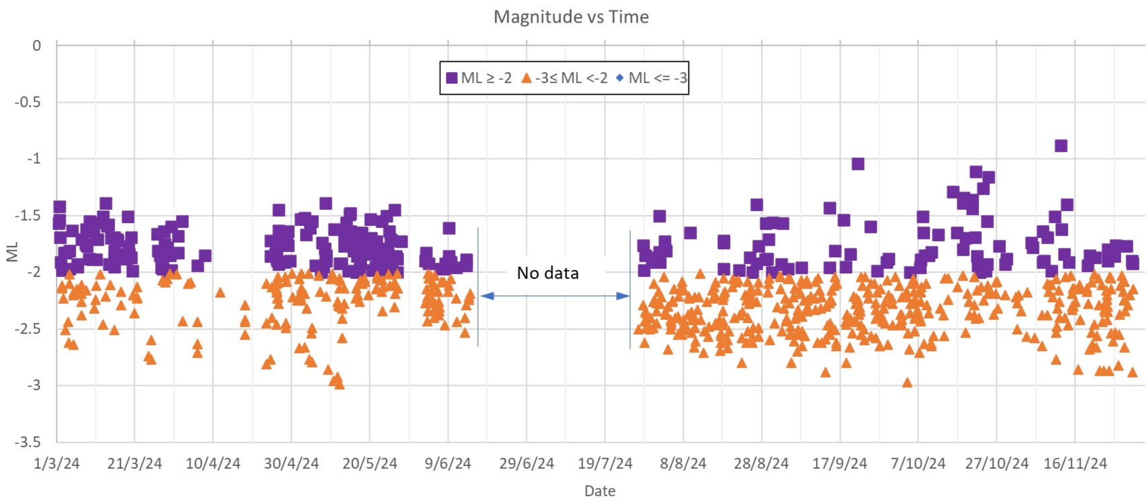


**Figure 9 Estimated local magnitude of seismic events with time**

## 3.3 Migration of clusters of seismic events

Figure 10 shows the spatial distribution of microseismic events recorded during two representative months: March (early in the monitoring period) and November (late in the monitoring period). In isometric view, event clusters were found to closely align with the inferred cave geometry, consistent with the seismogenic zone defined in the conventional caving model (Figure 1). In plan view, seismicity was predominantly concentrated above the cave footprint. These correspondences support the reliability of the event locations derived from the DAS monitoring system.

The southwest-looking view (Figure 10a) indicates a clear upward migration of the main event cluster and the upper boundary of the seismogenic zone. In contrast, the lower boundary exhibits little to no upward movement in the northern portion of the cave. The plan view distribution of seismicity (Figure 10b) further shows a noticeable change in event clusters over time. These observations suggest uneven cave propagation, likely influenced by rock mass heterogeneity and site-specific mining conditions.

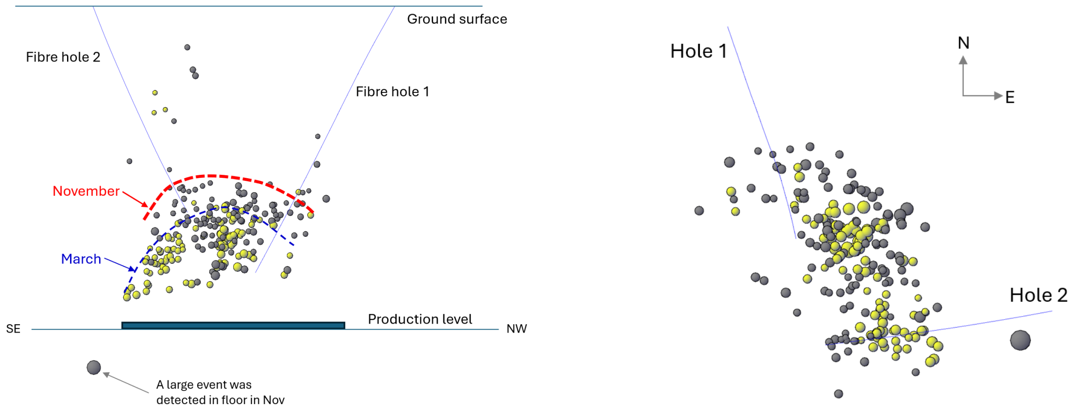


(a) (b)

**Figure 10 Spatial distribution of microseismic events recorded in March (yellow circles) and November (grey circles) 2024. (a) Southwest-looking view comparing the upper boundary of the seismogenic zone. (b) Plan view showing a sparse distribution of seismicity across the cave in November**

# 4 DSS results

The continuous strain sensing along the fibre-optic cable was intended to detect deformation zones and their location evolution to complement interpretations of caving activities and propagation. Figure 11 shows the strain changes recorded along the two boreholes relative to their initial (reference) measurements.

No significant strain changes were detected along the fibre cable installed in Hole 1 (Figure 11a). This result was not surprising, as the bottom end of the DSS cable is located at 50 m from the cave boundary. At the time of installation, the cave had already broken through to the expected final position of the hole on the edge of the cave. The monitored results confirm that the rock mass intersected by this borehole remained largely undeformed during the monitoring period.

In contrast, Hole 2 at the time of installation had not been broken through by the final predicted intersection. Over the monitoring period, microstrain of up to 700 με was detected along this cable (Figure 11b) and strain change along the length of the cable exhibited two patterns:

- The lower section of the borehole (410–440 m) showed a contiguous strain response, consistent with rock mass deformation within the yielded zone.
- The middle section of the borehole (200–370 m) showed intermittent strain changes, with values ranging from 200 to approximately 700 με. This discontinuous response is interpreted as deformation possibly within the seismogenic zone or the elastic zone, where partial stress release may induce delamination or slip along pre-existing fractures.

Although a complete strain evolution throughout the caving process was not observed within the monitoring period, the results demonstrate the capability of DSS to provide valuable deformation information that complements conventional geotechnical monitoring.

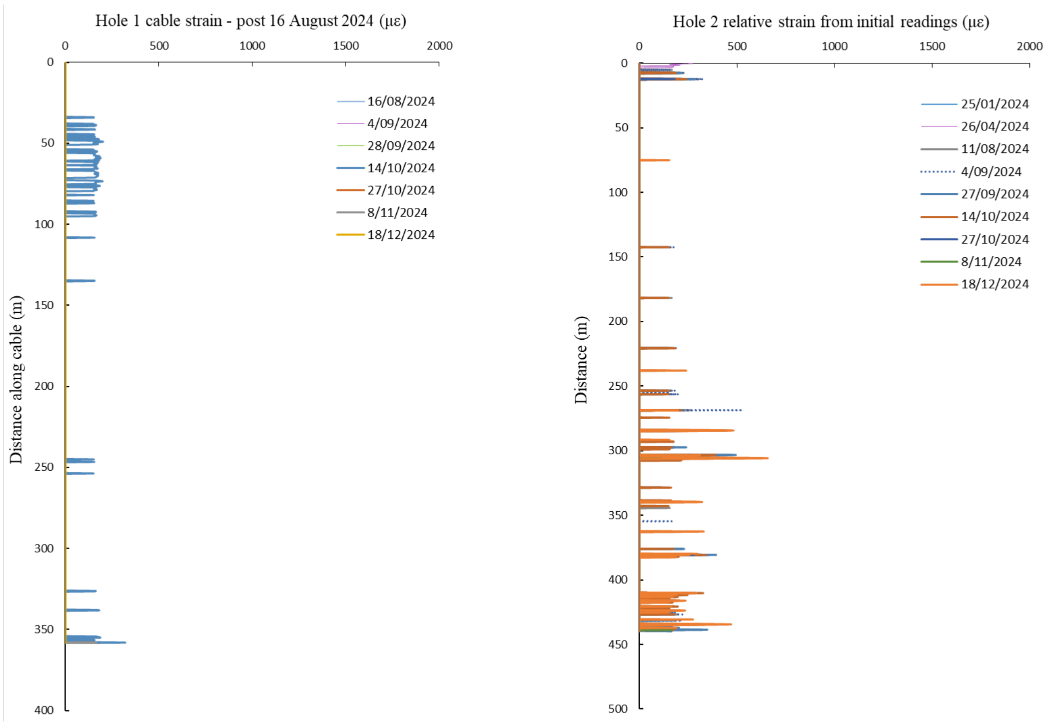


(a) (b)

**Figure 11 DSS monitored strain change along the two instrumentation boreholes; (a) Hole 1; (b) Hole 2**

# 5 Detecting response of a highly fractured zone

DAS has the potential for improving the ability to capture both seismic and aseismic phenomena when integrated with conventional geophone seismic systems (Dande et al. 2024). At the study mine, an approximately 150 m-thick highly fractured zone overlies the orebody and is expected to behave largely aseismically. The DAS data were therefore examined in detail to explore whether deformation-related signals could be identified within this broken zone. As a result, two distinct waveform types of seismic triggers were recognised.

The first type (Figure 12) displays clear signal amplitudes, and in many cases, was detected by fibre in only one borehole. These events have estimated local magnitudes in the range of −3 to −2 and can be located using the DAS-geophone network. As previously explained, the surface fibre cable was subjected to strong noise interference. To avoid the multi-solution issue in source location, the surface triaxial geophone (G3) installed near the borehole was also used for source location. The three-dimensional layout of triaxial geophones and fibre cables installed in the boreholes is shown in Figure 12b. Figure 13 shows the location of detected seismic events in the fractured zone in cross-section.

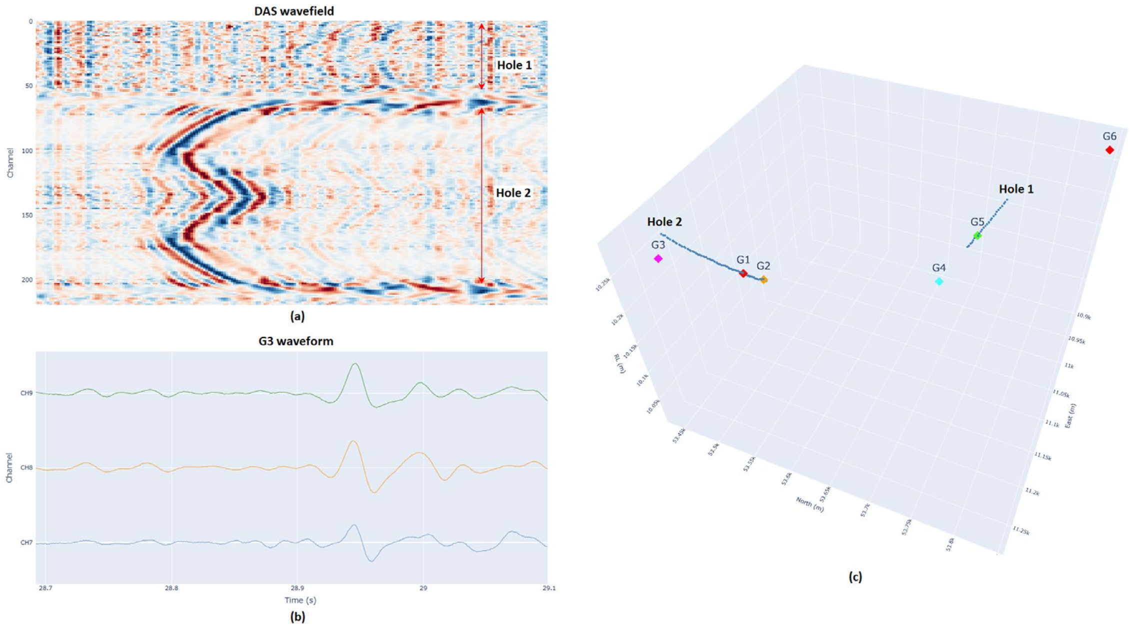


**Figure 12 (a) Example of DAS wavefield associated with the weak event; (b) Related waveform recorded by the triaxial geophone G3 installed on the surface near Hole 2; (c) 3D location of the borehole fibre cables and triaxial geophones. The sensing channels along the fibre cables and geophones are denoted by blue dots and diamonds, respectively**

A plausible source mechanism for these microseismic events is shear failure of large broken rock blocks or the collapse of interlocked rocks under certain locking mechanisms. Despite low intact cohesion, discrete rock blocks within the broken zone may be interlocked or arched under high clamping forces. As the cave back propagates towards the overlying weak zone, increasing tangential stresses may cause shear movement between the rock blocks and further propagation of fractures. Failures of these stressed structures could generate seismic energy; however, the limited energy of these events likely constrains wave propagation through the fractured rocks, resulting in detection by fibre cables only in close proximity.

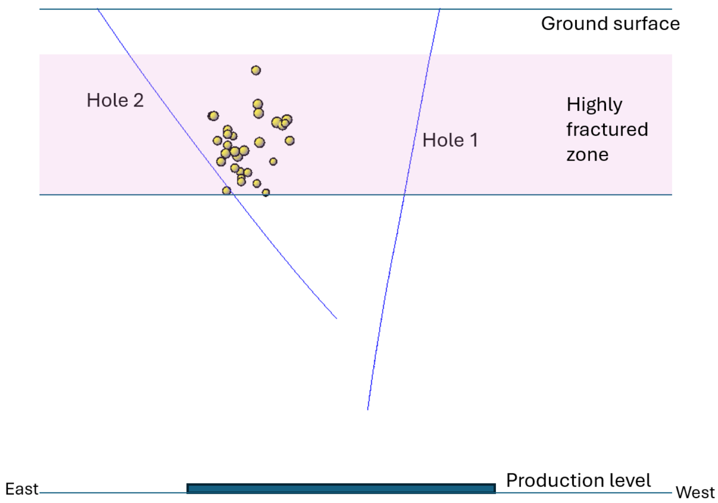


**Figure 13 Locations of weak seismic events captured by the DAS network in cross-section**

The second type of response (Figure 14) was recorded only over short fibre sections for very short durations, with no identifiable shear-wave arrivals. These signals likely related to aseismic near-field rock movements in the broken zone, such as localised sliding along pre-existing fractures or intra-block fracturing with minimal seismic radiation. These events were in close proximity to the fibre, and their depth can be inferred from the responding DAS channel numbers.

Although the number of detected events is insufficient to fully characterise fracturing activities within the broken zone, their spatial and temporal distributions are still informative, particularly when integrated with other monitoring data such as surface subsidence and open hole dipping inspections. In mines with a broken or failed rock mass layer or crown pillar, the ability to detect both seismic and aseismic deformation would be valuable for assessing overall cave stability (including chimney caving) and evaluating the potential for subsidence-related hazards.

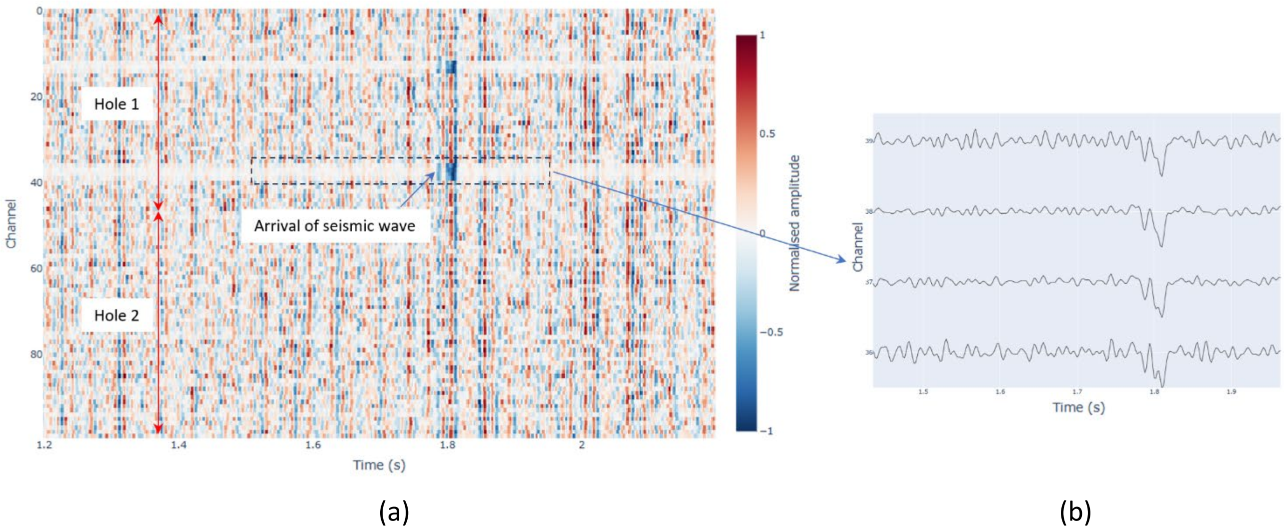


**Figure 14 Likely aseismic localised fracturing events captured by only a small section of fibre in one hole. (a) DAS wavefield; (b )Zoomed-in view of waveforms of the channels with recorded this event**

# 6 Conclusion

A field experiment was conducted at a cave mine to evaluate the performance of an integrated DAS-DSS system for monitoring caving/fracturing propagation. Two types of fibre-optic cables were installed in inclined surface boreholes and a surface trench, with borehole and surface geophones used for microseismic calibration. Monitoring data were acquired and analysed over a period of over 10 months.

The DAS system recorded seismicity associated with caving and fracturing, with event locations and characteristics consistent with typical rock mass behaviour models. The DAS data were able to delineate the seismogenic zone and its extent, providing valuable insights into caving activities. In addition, DAS captured low-energy fracturing activities from a broken zone, offering additional data for assessing rock mass behaviours potentially associated with caving anomalies.

The DSS system detected only limited strain changes, likely due to the short monitoring duration and the borehole position relative to the active caving zone. Nevertheless, the results showed distinct strain patterns in the vertical direction that are consistent with accepted subsidence development mechanisms (Duplancic & Brady 1999). The DSS data are complementary to seismic observations in interpreting caving dynamics.

Overall, the integrated DAS-DSS approach demonstrated excellent capability for continuous monitoring of rock mass fracturing and deformation. It can be used to complement existing cave monitoring systems, particularly where existing boreholes can be re-used following their primary purposes. While DAS provides valuable information on fracturing development and seismogenic zone evolution, DSS offers contiguous measurement of deformation. Together, they can enable an improved understanding of caving behaviours.

The study has also highlighted several challenges in the application of fibre-optic sensing for caving monitoring. The primary challenge arises from the inherent limitation of DAS, including its insensitivity to seismic wave propagating perpendicular to fibre orientation and the current immaturity of methods for processing large volume of data to enable real-time seismic event location. These challenges have constrained its use to qualitative assessment of caving behaviour under defined monitoring goals, rather than providing timely operational decision support. Furthermore, effective interpretation of the monitoring results into actionable insights requires integration of expertise across fibre-optic sensing, caving mechanics and geology, which can impede its broad application.

Building on experience from this and other field studies, and leveraging advances in machine learning, the CSIRO research team has made significant progress in developing robust and efficient data processing algorithms. Continued advancement and field validation are expected to significantly improve practicality and reduce overall costs to facilitate more applications in mining.

# Acknowledgement

We are deeply grateful to the host mine and the geotechnical team for accommodating this field experiment.

# References

Dande, S, Forbes, E, Butler, T, Graham, K, Hawryluck, C, Hall, A, … Cherubini, A 2024, 'Utilising distributed acoustic sensing for monitoring rock mass stress conditions in underground mining: a case study', in P Andrieux & D Cumming-Potvin (eds), *Deep Mining 2024: Proceedings of the 10th International Conference on Deep and High Stress Mining,* Australian Centre for Geomechanics, Perth, pp. 375–390, https://doi.org/10.36487/ACG_repo/2465_19

du Toit, JH, Goldswain, G, Oliver, G 2022, 'Can DAS be used to monitor mining induced seismicity?', *International Journal of Rock Mechanics & Mining Sciences*, vol. 155, 10512.

Duan, Y, Luo, X, van de Werken, M, Dean, P, & Elmouttie, M 2023, 'Numerical investigation of seismic source location using distributed acoustic sensing for rockfall monitoring', in PM Dight (ed.), *SSIM 2023: Third International Slope Stability in Mining Conference*, Australian Centre for Geomechanics, Perth, pp. 639–646, https://doi.org/10.36487/ACG_repo/2335_42

Duan, Y, Shen, B, Luo, X, van de Werken, M, Harpley, D & Lin X 2025, 'Application of distributed acoustic sensing for caving mechanisms assessment at an underground longwall coal mine', paper presented at Bowen Basin Symposium, Mackay, 15–17 September 2025.

Duplancic, P & Brady, BH 1999, 'Characterisation of caving mechanisms by analysis of seismicity and stress', paper presented at the 9th ISRM Congress, Paris, August 1999.

John, D & Hoehn, K 2024, 'Distributed fibre optic sensing for ground monitoring in underground hard rock mining', in P Andrieux & D Cumming-Potvin (eds), *Deep Mining 2024: Proceedings of the 10th International Conference on Deep and High Stress Mining*, Australian Centre for Geomechanics, Perth, pp. 391–402, https://doi.org/10.36487/ACG_repo/2465_20

Luo, X & Duan, Y 2021, 'Microseismic monitoring of longwall caving process using distributed optic fibre sensing', paper presented at the 55th U.S. Rock Mechanics/Geomechanics Symposium, virtual, June 2021.

Sainsbury B 2012, *A Model for Cave Propagation and Subsidence Assessment in Jointed Rock Masses*, PhD thesis, University of New South Wales, Sydney.

Xie, JL, Qu, QD, Zhu, WB, Wang, XZ, Xu, JL, Ning, S, Hou, T & Luo, X 2023, 'Distributed strain monitoring of overburden delamination propagation at a deep longwall mine', *International Journal of Rock Mechanics & Mining Sciences*, vol. 171, 105589.